Journal of Thermal Analysis and Calorimetry (2025) 150:10595–10608
https://doi.org/10.1007/s10973-025-14361-y

Life cycle cost and carbon footprint analysis of CuO–Al_2O_3/water hybrid nanofluids in thermoelectric vaccine refrigerators

Pinar Mert Cuce[1,2,3] · **Tamer Guclu**[4,5] · **Erdem Cuce**[5,6,7]

Received: 30 November 2024 / Accepted: 27 April 2025 / Published online: 3 June 2025

Abstract

This study investigates the application of a CuO–Al_2O_3/water hybrid nanofluid as a coolant in thermoelectric vaccine refrigerators, aiming to enhance heat dissipation from the Peltier module's hot side. A 35-L cooling cabinet was utilised, and experimental comparisons were made using water and a 2% CuO–Al_2O_3/water hybrid nanofluid. Results show that the vaccine cabinet reaches the target temperature of 4 °C in 990 s with nanofluid, compared to 1200 s with water. The system's energy consumption was reduced by 18.3%, and carbon emissions decreased by 12.3% over a 15-year lifespan, highlighting its environmental benefits. Despite similar coefficients of performance (COP), the nanofluid system demonstrates enhanced efficiency, shorter cooling times, and long-term sustainability advantages. These findings support the adoption of hybrid nanofluids in thermoelectric cooling applications for energy-efficient and environmentally friendly refrigeration systems.

Keywords Thermoelectric cooling · CuO–Al_2O_3 hybrid nanofluid · Vaccine refrigeration · Life cycle cost analysis (LCCA) · Carbon footprint reduction

Introduction

As global industrialisation continues to expand, energy demands are rising rapidly, and a lot of electrical energy is used in the cooling and cold transportation of products such as medicines and organs, around the world. Although vapour compression systems are widely used in these applications, there have been many attempts to use thermoelectric devices instead of vapour compression systems, especially in recent decades [1, 2]. The most important reasons for preferring thermoelectric devices are that they operate silently and without vibration and that they do not require extra costly equipment such as compressors and valves [3]. Thermoelectric devices can be classified into two classes: thermoelectric generators (TEGs), which operate according to the Seebeck effect and enable electricity generation from the temperature difference between the surfaces [4]. The other one is thermoelectric coolers (TECs), which operate according to the Peltier effect. The Peltier effect is the phenomenon, whereby a circuit is created with two semiconductors, *P* and *N*-type, and when current is applied to the circuit, one surface of the TEC cools and the other surface heats [5]. As shown in Fig. 1, the *P* and *N*-type element pairs are connected as electrical and thermal in series and parallel, respectively, and placed between two ceramic plates. A

✉ Erdem Cuce
erdem.cuce@erdogan.edu.tr

1 Department of Architecture, Faculty of Engineering and Architecture, Recep Tayyip Erdogan University, Zihni Derin Campus, 53100 Rize, Turkey

2 College of Built Environment, Birmingham City University, Birmingham B4 7XG, UK

3 Centre for Research Impact and Outcome, Chitkara University Institute of Engineering and Technology, Chitkara University, Rajpura, Punjab 140401, India

4 Department of Mechanical Engineering, Faculty of Engineering, Bayburt University, Dede Korkut Campus, 69000 Bayburt, Turkey

5 Department of Mechanical Engineering, Faculty of Engineering and Architecture, Recep Tayyip Erdogan University, Zihni Derin Campus, 53100 Rize, Turkey

6 University Centre for Research and Development, Chandigarh University, Mohali, Punjab 140413, India

7 Center for Research Impact and Outcome, Chitkara University, Rajpura, Punjab 140401, India

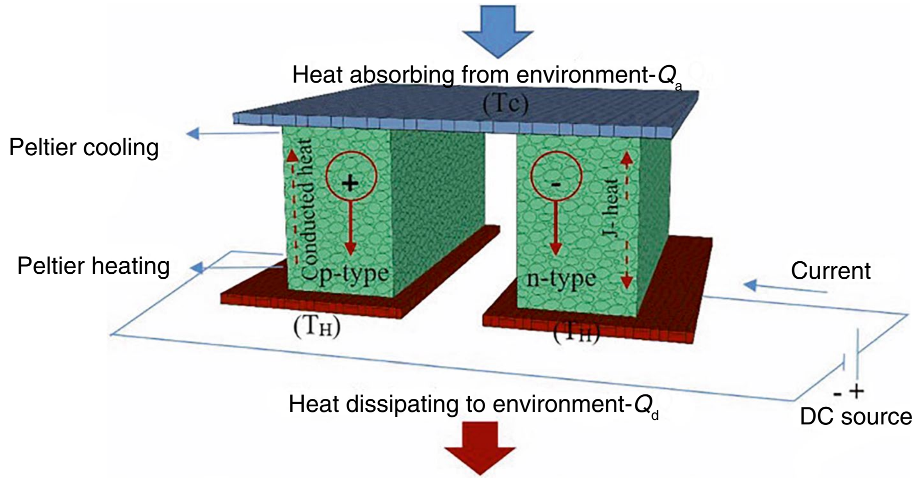

Fig. 1 Working principle of TECs [6]

difference in temperature is observed on the TEC surfaces with the application of current to the circuit [6].

Thanks to their low energy costs, easy installation, suitability for automation, compact structure, and lightweight, these devices are widely used in many applications, from mini refrigerators to electronic circuit cooling applications [7]. However, COP values are lower than conventional cooling devices [8]. Therefore, studies are conducted to enhance the COP values of these devices. The most effective way to enhance the COP values of TECs is to keep the temperature of the hot surface of TECs at low degrees. Various techniques are applied for this purpose [9]. The most common techniques include air-to-refrigerant fluid systems, air-to-air systems with forced convection using fans and air-to-air systems with natural convection [10]. Air-cooled systems operate quieter and require less equipment. However, their cooling performance has been shown to be lower than air–liquid systems. Afshari [11] carried out a numerical and empirical study to observe two different thermoelectric cooler modes. In the air-to-air configuration, the TEC device was equipped with heatsinks and fans on surfaces, while the air-to-water setup utilised a pump and water-cooled unit in refrigerators made from styrofoam sheets. Therefore, using liquid to dissipate waste heat in TEC systems could be a more efficient option. The results revealed that the air-to-water mode was more efficient, with a COP approximately 30–50% higher than the air-to-air configuration. Huang et al. [12] analysed the thermal characteristics of a water-cooled thermoelectric device for electronic applications. The effects of heat load and electric current on the cooling efficiency of the device were determined both experimentally and theoretically. The experimental results show that integrating the thermoelectric cooler with a water-cooling device significantly enhances thermal performance at heat loads under 57 W. Afshari et al. [13] analysed the performance of air-to-water TECs to optimally evaluate double TEC systems and compare them with single TECs. Two-stage TECs were examined, and the desired values were obtained for comparison across several parameters. The experimental results showed that the single Peltier device achieved the highest COP, approximately 25% higher than that of the binary discrete systems. Consecutive binary Peltier systems were also found to have the lowest COP, indicating significantly reduced performance. Pathak et al. [14] examined the variation in temperature over time for a water-cooled thermoelectric setup, where a TEC was employed to cool the cabinet. The current was adjusted between 5 and 11A, and the time required for the temperature to drop from ambient to 10–15 °C was recorded. The results revealed that the most significant temperature decrease in the polystyrene cabinet occurred when the current was set at 50% of the maximum current. In order to further increase the thermal conductivity, nanofluid is also used instead of base fluid on the hot surface of the TEC. Nanofluids are obtained by adding various nanoparticles to the base liquid and applying certain processes. In general, their thermal conductivities are higher than the base fluids from which they are obtained [15]. There are many studies showing that nanofluids increase thermal conductivity [16–20]. Elibol et al. [21] investigated the integration of a TEC with two microchannel heat sinks using a TiO_2-water nanofluid to enhance cooling efficiency. Through experimental analysis, the thermal performance of the system was evaluated at different flow rates, comparing pure water and nanofluid. The results demonstrated that the Nusselt number increased with flow rate, and the COP significantly improved as the nanoparticle concentration rose. The study highlights the system's potential for electronic cooling, especially at low flow rates and higher nanoparticle concentrations. Cuce et al. [22] explored the effects of using nanofluids in TECs on thermal performances and COP values through detailed experiments. A water-cooled unit was placed on the Peltier's hot side, and an air-cooled heat exchanger was integrated for the purpose of cooling heated water. Different nanoparticles at concentrations of 0.1%, 0.5%, and 1% were added to the water, and temperature differences were measured under various ambient temperatures. Additionally, the cooling effect on the inside of the cooled cabinet was observed to simulate a load condition. The study found that the best temperature improvement of 26% occurred with 1% Al_2O_3 at 30 °C in no-load conditions. The most significant cooling performance 55.1% was achieved using 1% Al_2O_3–water nanofluid for the cooled water. Despite a slight decrease in the COP, the TEC system with nanofluids demonstrated substantial advantages over traditional water-cooled systems, notably improving cabinet cooling. As a continuation of this study, they examined the thermal performance of hybrid nanofluids containing Al_2O_3–TiO_2–SiO_2 nanoparticles were tested, and their performance was compared to water without nanoparticles. The results showed that nanofluids outperformed the reference case in all tests, with system efficiency improving as nanoparticle concentration increased. However, due to the Peltier effect, the COP was slightly lower than the reference. The greatest improvement in temperature difference reached 30.3% under loaded conditions and 25.1% under unloaded conditions when using 2% Al_2O_3–TiO_2–SiO_2/water nanofluid [23]. Mohammadian and Zhang [24] modelled and analysed the effects of Al_2O_3–water nanofluids on the performance of thermoelectric modules using two micro-pin–fin heat exchangers on cold and hot surfaces. The findings reveal that at low Reynolds numbers, adding a small number of nanoparticles to the fluid on the hot side significantly boosts the COP and reduces total entropy generation. At higher Reynolds numbers, nanoparticles improve the COP and reduce entropy generation on the cold side. Additionally, while decreasing nanoparticle size has little impact at low Reynolds numbers, it significantly enhances COP and reduces entropy at high Reynolds numbers on the cold side but shows an opposite effect on the hot side. Ahammed et al. [25] experimentally examined the performance of thermoelectric cooling for electronic devices using a multiport mini-channel heat exchanger with Al_2O_3–water nanofluids as the coolant. Nanofluids with different volume concentrations of Al_2O_3 were used to cool the hot side of the TEC, and the different Reynolds numbers. The results showed a 40% improvement in the COP with 0.2% nanofluid, along with a 9.15% reduction in the temperature difference between the hot and cold sides. This contributed to better cooling capacity. Duan et al. [26] experimentally investigated the heat transfer properties of Carbon Nanotube and Al_2O_3 nanofluids in a natural circulation loop for a thermoelectric cooler-based personal cooling system. Findings revealed significant heat transfer enhancements, providing insights useful for advancing personal cooling systems using thermoelectric refrigeration. Elibol [27] investigated the enhancement of thermal performances of TEC systems by integrating a ZnO–TiO_2/water hybrid nanofluid into a dual microchannel heat sink. The system was tested under varying nanofluid concentrations and flow rates to maximise performance. Key findings include a significant increase in heat transfer rates on both the heat-absorbing and heat-emitting sides as the nanofluid concentration increased from 0 to 0.03%, with a concurrent decrease in flow rate.

This study investigates the use of CuO–Al_2O_3/water hybrid nanofluid as a coolant in thermoelectric vaccine refrigerators. CuO–Al_2O_3/water hybrid nanofluid was selected as the coolant due to the thermal properties. Al_2O_3 nanoparticles are widely used because of their chemical stability, low cost, and non-toxicity, while CuO nanoparticles offer superior thermal conductivity. The combination of these two materials in a hybrid formulation has been shown an enhancement in thermal performance, resulting in higher heat transfer coefficients compared to single-component nanofluids. Furthermore, hybrid nanofluids based on CuO–Al_2O_3 have demonstrated better dispersion stability and lower sedimentation rates, which are critical for long-term operation in thermoelectric cooling systems. Compared to other alternatives such as TiO_2 or CNT-based nanofluids, CuO–Al_2O_3/water nanofluids offer a balanced trade-off between performance, stability, cost, and safety, making them highly suitable for sensitive applications like vaccine refrigeration [28–30]. A thermoelectric cooling system was employed in a 35-L cooling cabinet, and a liquid-cooled block was used on Peltier's hot side device to remove heat from this surface with the help of the CuO–Al_2O_3/water hybrid nanofluid. This aims to enhance the heat dissipation from the hot surface of Peltier. Thanks to the effective heat dissipation from the hot surface of the TEC, the temperature of the vaccine cabinet is expected to reach lower temperature values more quickly, leading to reduced energy consumption. This study supports the efficient use of energy resources within cooling applications, with potential benefits for refrigeration and electronics cooling.

Material and method

Material

Preparation of hybrid nanofluid

In the study, CuO–Al_2O_3/water hybrid nanofluid with 2% nanoparticles by mass was used. The reason for choosing CuO and Al_2O_3 nanoparticles is that they have high thermal conductivity values [28–31]. While direct experimental measurements of thermal conductivity and viscosity were not conducted in this study, the CuO–Al_2O_3/water hybrid nanofluid used in the study has been extensively investigated in previous literature. Based on prior experimental studies, CuO–Al_2O_3 hybrid nanofluids at 2% concentration are known to exhibit significantly improved thermal

Table 1 Characteristics of nanoparticles [32]

Property	Al_2O_3	CuO
Purity	99.5%	99.9%
Size	78 nm	38 nm
Specific surface area /m^2g^{-1}	> 20	> 20
Morphology	Nearly spherical	–
Colour	White	Black
pH	–	7

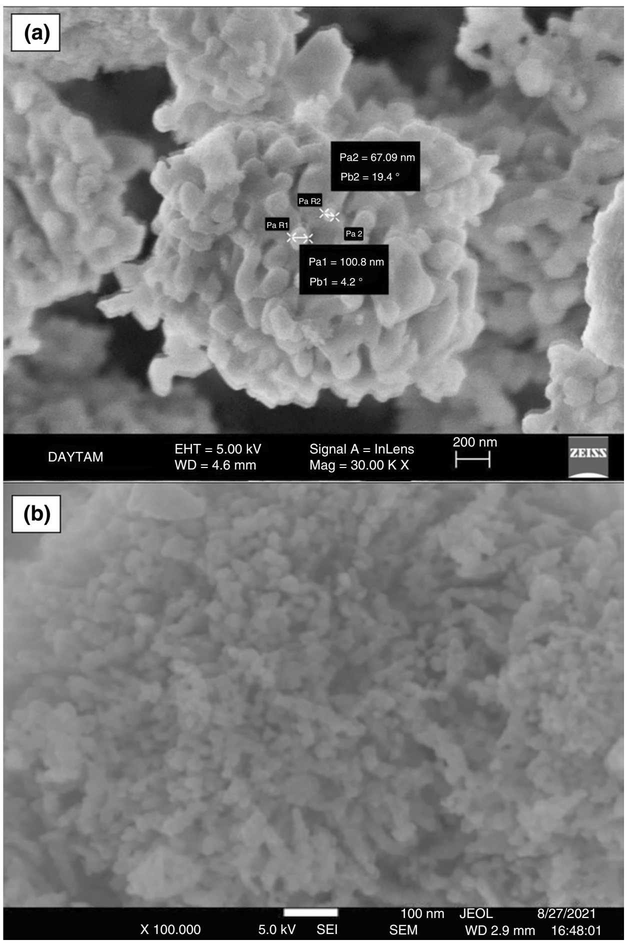

Fig. 2 SEM images of Al_2O_3 nanoparticles (**A**) and CuO nanoparticles (**B**) [32]

conductivity and moderate viscosity changes in the temperature range of 25–40 °C. These improvements are crucial in enhancing heat transfer and ensuring the stability of the flow within thermoelectric cooling systems [25, 26]. The characteristic properties of the nanoparticles obtained from Nanografi company are shown in Table 1, and the SEM images are shown in Fig. 2.

The cooling performance increase obtained by using CuO–Al_2O_3/water hybrid nanofluid is based on several basic physical mechanisms in the fluid. The most important of these is Brownian motion; that is, the random and continuous movement of nanoparticles in the liquid. This movement causes micro-level mixing and local convection in the liquid, allowing heat to be distributed more effectively. In addition, thermophoresis (particle migration under the influence of heat) occurs from hot regions to cold regions, which contributes to more efficient heat transfer. The liquid molecule layers formed around the nanoparticles change the local thermal conductivity of the liquid. In addition, the interactions between CuO and Al_2O_3 particles and the micro-convection currents they create increase the total heat transfer capacity of the nanofluid. These mechanisms work together to increase the effective thermal conductivity of the nanofluid, thus removing heat from the hot surface of the Peltier module more quickly and reaching the target temperature in a shorter time [33–35].

The nanofluid was prepared by adding Al_2O_3 and CuO nanoparticles to 1 kg of deionised water at certain values. An ultrasonic homogenizer was used to obtain nanofluids. The nanoparticles were weighed with a precision scale and added to the base fluid. Then, they were mixed for 1 h at 400 W 24 kHz with the help of an ultrasonic homogenizer. Thus, the experiments were completed without sedimentation during the experiments. The preparation stages of the nanofluids are shown in Fig. 3.

Preparation of cooling cabinet

The cooling cabinet was designed to be portable, lightweight, and particularly suitable for use as a vaccine refrigerator. With this aim, a cabinet with a thickness of 6 mm was manufactured with 2-mm-thick XPS insulation material in three layers. The cooling cabinet has internal dimensions of 500 mm in height, 200 mm in depth, and 350 mm in width, with a capacity of 35 L. These dimensions were specifically chosen to make the cabinet suitable for portable vaccine cabinet applications. The manufacturing stages of the cooling cabinet are shown in Fig. 4.

Preparation of TEC system

A single-stage Peltier module (TEC1-12712) with 12 V and 12 A capacity has been used in the system. The specifications of the Peltier module are presented in Table 2.

An aluminium heatsink has been attached to the cold side of the Peltier module using thermal paste. A fan is mounted on the other side of the aluminium heatsink to accelerate heat transfer. On the hot surface of the TEC, a liquid-cooled block has been attached with thermal paste. Another aluminium heatsink and fan are mounted on the other side of the liquid-cooled block as well. The setup of the Peltier module is shown in Fig. 5.

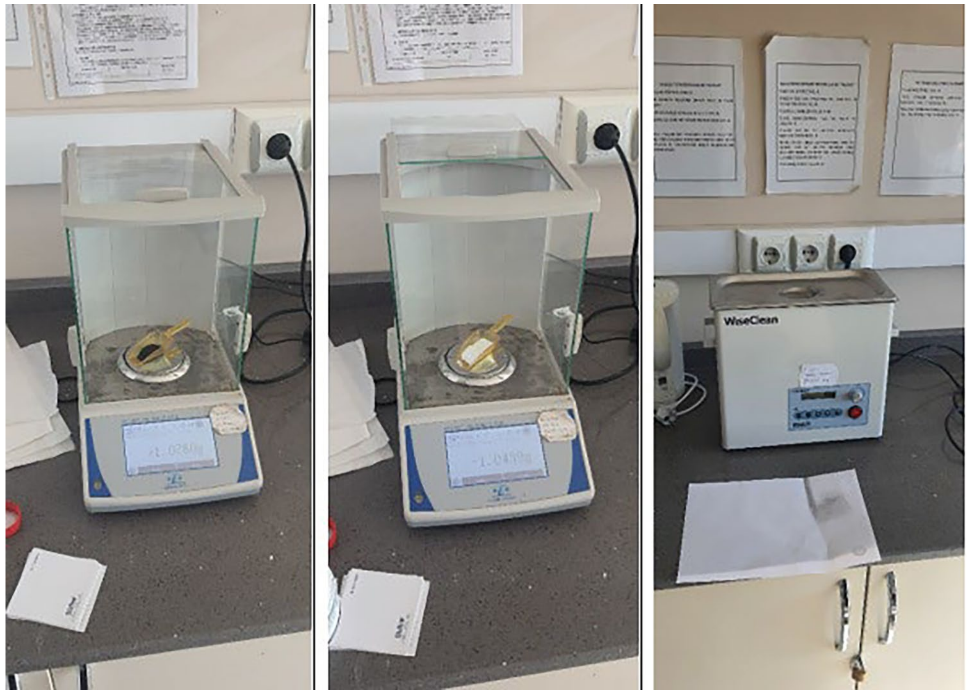

Fig. 3 Preparation of nanofluid

Fig. 4 Manufacturing of cooling cabinet

Table 2 Specification of TEC1-12712

T_h/°C	ΔT_{max}/°C	U_{max}/Voltage	I_{max}/amps	Q_{cmax}/watts	AC resistance/ohms	Tolerance/%
27	70	16	11.5	115.2	1.1	± 10
50	79	17.2	11.5	125.8	1.21	

Method

The Peltier device is integrated into the vaccine refrigerator at the middle of its side surface. An air-cooled heat exchanger is used to dissipate the heat absorbed by the hybrid nanofluid from the hot surface of the TEC into the environment. A fluid reservoir and a pump are also incorporated into the system to ensure fluid circulation. The CuO–Al_2O_3/water hybrid nanofluid is pumped to the liquid-cooled block on the hot surface of the TEC, where it absorbs heat. The heated nanofluid then enters an air-cooled heat exchanger, where it releases its heat to the surroundings. The cooled nanofluid returns to the fluid

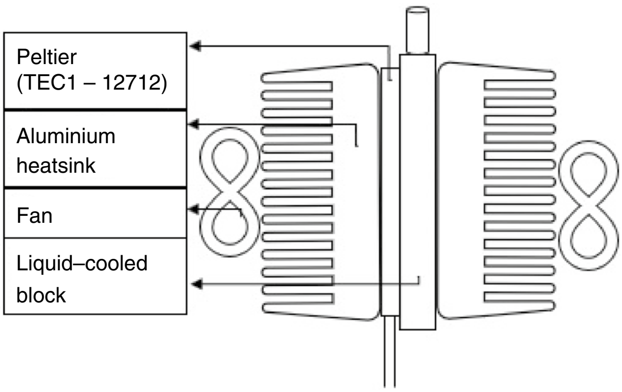

Fig. 5 Setup of the Peltier module

reservoir and is then pumped back to the liquid-cooled block, completing the fluid cycle. The experimental setup is shown in Fig. 6.

K-type thermocouples were used for the purpose of measuring the vaccine refrigerator temperature, cold fin temperature, hot fin temperature, coolant temperature, and ambient temperature.

The cooling power (Q_c) and COP values were calculated from the experimental data using the following equations [33, 36, 37]:

$$Q_c = \mathrm{Se}T_cI - \frac{1}{2}I^2R - k(T_h - T_c) \tag{1}$$

where Se represents the Seebeck coefficient. R, T_h and T_c represent the electrical resistance of thermoelectric, temperatures of sides of Peltier, respectively. I, and k represent the current and thermal conductivity of Peltier.

$$\mathrm{COP} = \frac{Q_c}{P_e} \tag{2}$$

$$P_e = \mathrm{VI} \tag{3}$$

Life cycle cost analysis

Life cycle cost analysis (LCCA) is a method that evaluates all costs incurred throughout the entire life cycle of a product, project or system (planning, design, construction, operation, maintenance and demolition/recycling) [38]. LCCA considers not only initial investment costs, but also long-term costs such as energy costs, operation and maintenance costs, repair costs, replacement costs and demolition/recycling costs. Therefore, LCCA is used to determine the most economically viable option among different alternatives, to make budget planning, to provide risk management, to improve decision-making processes and to facilitate performance monitoring [39]. LCCA can be applied in many different areas such as building design and construction, energy systems, transportation systems, infrastructure projects and product development. In general, the following formula is used when performing LCCA:

$$\mathrm{LCC} = P + \sum_{t=1}^{N} \frac{Q_t}{(1+r)^t} \tag{4}$$

Here, P represents the initial insulation cost, Q_t represents the annual operation, maintenance and energy costs, N represents lifetime (year), t represents the determined operation cost year, and r represents the discount rate [40].

Carbon footprint analysis

Carbon footprint analysis is a method of measuring the environmental impact of a product, service, organisation, or individual in terms of greenhouse gas emissions [41]. These emissions are usually expressed as carbon dioxide equivalent (CO_{2e}) and include all greenhouse gases that contribute to global warming. Carbon footprint analysis helps us understand

Fig. 6 Experimental setup

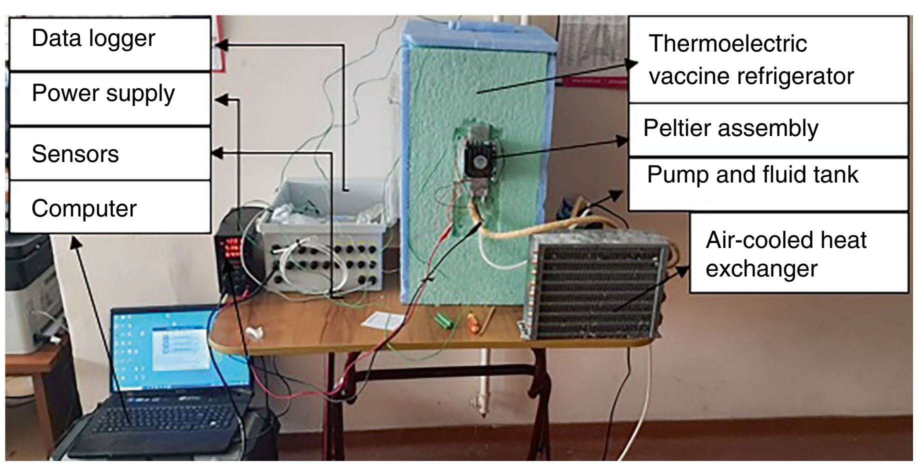

the impact of our activities on the planet [42]. This information allows us to develop strategies to reduce greenhouse gas emissions [43]. It is also an important tool in achieving sustainability goals. Businesses and individuals can fulfil their environmental responsibilities by reducing their carbon footprint [44].

$$\text{Carbon Emission}\left(\text{kgCO}_2\right) = \text{Annual Energy Consumption(kWh)} \times \text{Emission Factor} \quad (5)$$

$$\text{Total Carbon Footprint}\left(\text{kgCO}_2\right) = \sum_{t=1}^{N} \text{Annual emission}\left(\text{kgCO}_2\right) \quad (6)$$

Uncertainty analysis

The total uncertainty can be calculated as follows:

$$W_{\mathrm{Q}} = \left[\left(\frac{\partial Q}{\partial X_1} \times W_1\right)^2 + \left(\frac{\partial Q}{\partial X_2} \times W_2\right)^2 + \left(\frac{\partial Q}{\partial X_{\mathrm{n}}} \times W_{\mathrm{n}}\right)\right]^{\frac{1}{2}} \quad (7)$$

Here, Q denotes the dimension to be measured, X denotes the variable affecting the measurement, and W denotes the uncertainty of the independent variable [45].

For the case where uncertainty analysis is performed,

- Se = 0.05
- T_{c} = 271.65 K
- I = 6 A
- R = 0.8 Ω
- k = 0.48 W K^{-1}
- T_{h} = 295.05 K

$$\begin{aligned} Q_{\mathrm{c}} &= (0.05*271.65*6) - (0.5*6*6*0.8) - (0.48*(295.05 - 271.65) \\ Q_{\mathrm{c}} &= 55.863\ \mathrm{W} \end{aligned} \quad (8)$$

$$\begin{aligned} W_{Q_{\mathrm{c}}} &= \left[\left(\frac{\partial Q}{\partial T_{\mathrm{c}}} \times 0.1\right)^2 + \left(\frac{\partial Q}{\partial I} \times 0.1\right)^2 + \left(\frac{\partial Q}{\partial T_{\mathrm{h}}} \times 0.1\right)^2 + \left(\frac{\partial Q}{\partial R} \times 0.01\right)^2 + \left(\frac{\partial Q}{\partial k} \times 0.01\right)^2\right]^{\frac{1}{2}} \\ &= \left[(0.78 \times 0.1)^2 + (8.78 \times 0.1)^2 + (-0.48 \times 0.1)^2 + (-18 \times 0.01)^2 + (-23.4 \times 0.01)^2\right]^{\frac{1}{2}} \\ &= 0.93 \end{aligned} \quad (9)$$

$$P_{\mathrm{e}} = \mathrm{VI} = 12*6 = 72\ \mathrm{W} \quad (10)$$

$$\frac{\partial P_{\mathrm{e}}}{\partial V} = \mathrm{I} = 6 \quad (11)$$

$$\frac{\partial P_{\mathrm{e}}}{\partial I} = \mathrm{V} = 12 \quad (12)$$

$$\begin{aligned} W_{P_{\mathrm{e}}} &= \left[\left(\frac{\partial P_{\mathrm{e}}}{\partial V} \times 0.1\right)^2 + \left(\frac{\partial P_{\mathrm{e}}}{\partial I} \times 0.1\right)^2\right]^{\frac{1}{2}} \\ &= \left[(\times 0.1)^2 + (12 \times 0.1)^2\right]^{\frac{1}{2}} = 1.34 \end{aligned} \quad (13)$$

$$\mathrm{COP} = \frac{Q_{\mathrm{c}}}{P_{\mathrm{e}}} = \frac{55.863}{72} = 0.78 \quad (14)$$

$$\frac{\partial \mathrm{COP}}{\partial Q_{\mathrm{c}}} = \frac{1}{P_{\mathrm{e}}} = \frac{1}{72} = 0.01 \quad (15)$$

$$\frac{\partial \mathrm{COP}}{\partial P_{\mathrm{e}}} = -\frac{Q_{\mathrm{c}}}{P_{\mathrm{e}}^2} = -\frac{-55.863}{(72)^2} = -0.01 \quad (16)$$

$$W_{\mathrm{COP}} = \left[\left(\frac{\partial \mathrm{COP}}{\partial \mathrm{Q_c}} \times 0.93\right)^2 + \left(\frac{\partial \mathrm{COP}}{\partial P_{\mathrm{e}}} \times 1.34\right)^2\right]^{\frac{1}{2}} = 0.02 \quad (17)$$

Consequently,

$$\mathrm{COP} = 0.78 \pm 0.02$$

Results

During the experiments, water and a 2% mass concentration CuO–Al_2O_3/water hybrid nanofluid were used as coolants, and the results obtained in both cases were compared. Initially, experiments were conducted using water as the coolant. Subsequently, the experiments were repeated under similar conditions using the nanofluid. Throughout the experiments, the vaccine refrigerator temperature, cold fin temperature, hot fin temperature, ambient temperature, and coolant temperature were measured. The time taken for the vaccine refrigerator to reach 4 °C was considered during the measurements. This is because vaccine storage conditions vary between 2 and 6 °C [46–48]. During the experiment, the voltage value was set to 12 V and power calculations were made by observing the current drawn by the system.

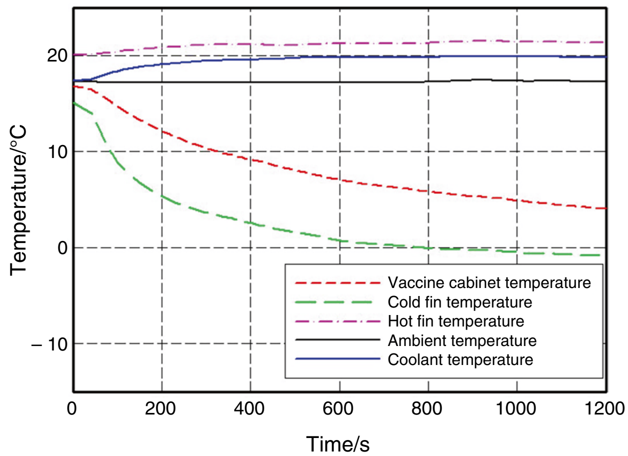

Fig. 7 Temperature changes for the case where water was used as the coolant

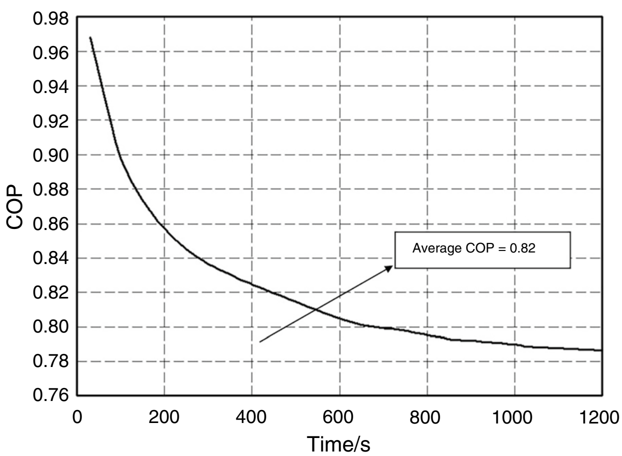

Fig. 8 COP changes for the case where water was used as the coolant

Cooling effect and COP assessment for TEC vaccine refrigerator

The temperature values obtained when using water as the coolant are shown in Fig. 7. As seen in Fig. 7, the vaccine refrigerator temperature drops to 4 °C, which is ideal for vaccine storage conditions, after 1200 s. During the experiments, it was observed that the system consumed 72 W of power. In addition, the system's mean COP value was found to be 0.82 for this determined period. The COP change is shown in Fig. 8.

In the case where CuO–Al_2O_3/water hybrid nanofluid is used as a cooling fluid in the system at a mixing ratio of 2% by mass, it is noticed that the temperature of the vaccine cabinet reaches 4 °C after 990 s. It is noticed that the temperature of the vaccine cabinet reaches the desired value in a shorter time by using nanofluid instead of water as a cooling fluid. The temperature data obtained in the experiments

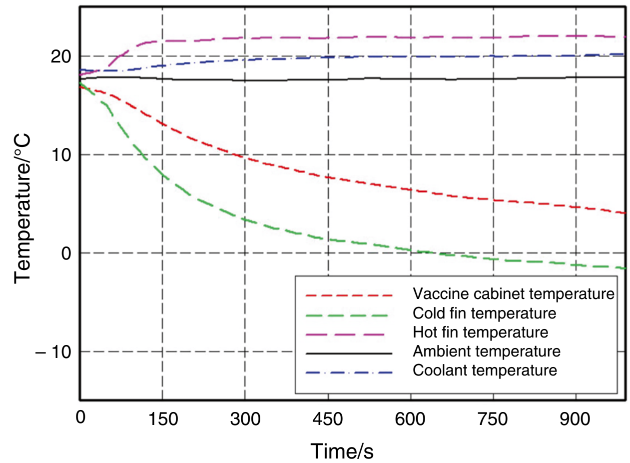

Fig. 9 Temperature changes for the case where CuO–Al_2O_3/water hybrid nanofluid was used as the coolant

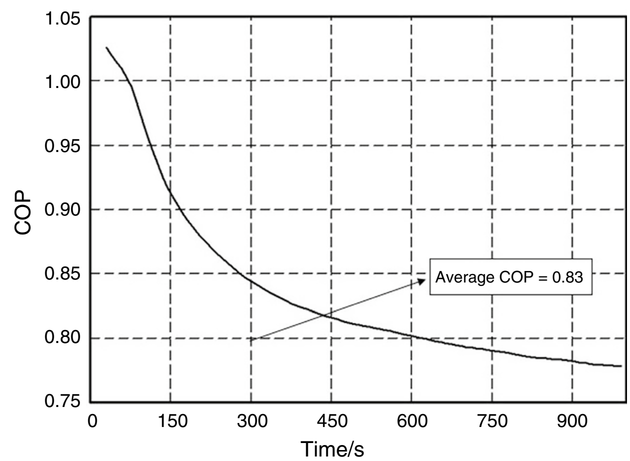

Fig. 10 COP changes for the case where CuO–Al_2O_3/water hybrid nanofluid was used as the coolant

carried out in the specified case are shown in Fig. 9. During the experiments, it was observed that the system consumed 58.8 W of power. In addition, the system's mean COP value was found to be 0.68 for this determined period. The COP change is shown in Fig. 10.

As can be seen, the COP values obtained in both cases are almost the same. In the case where CuO–Al_2O_3/water hybrid nanofluid is used, although the time it takes for the system to reach the desired temperature is shortened, the total energy consumption and cooling capacity ratio are observed to be quite close to the other system. In addition, since the current difference between the systems is small, it does not have a significant effect on the COP. In addition, the COP calculation in TECs depends on the temperature difference between the surfaces. Since the Peltier has almost reached its optimum operating conditions in both cases, the Dt values are close to each other. These reasons show that the COP values of the two systems are expected to be almost the same.

Although this study focused on evaluating the performance of hybrid nanofluid-supported thermoelectric cooling, it is also important to compare the obtained results with other advanced cooling technologies. For example, phase change materials (PCM) attract attention with their high energy density and passive operation properties, but they have disadvantages such as slow heat transfer and phase separation. Conventional liquid cooling systems, although they have high heat removal capacity, require additional components such as pumps and valves and have disadvantages in terms of portability. In contrast, the nanofluid-supported TEC system proposed in this study combines advantages such as compact structure, low energy consumption and environmentally friendly operation. In future studies, the competitiveness of the system can be evaluated more comprehensively by making direct performance comparisons with such alternative technologies.

LCCA assessment for TEC vaccine refrigerator

- **Cost Estimates:**

Total of about 2 m^2 of XPS insulation: ≈ $20.

- Peltier Element: Price varies greatly depending on the performance of the Peltier element. ≈ $20 for the TEC1-12712 used in the system.
- Water-cooled block: ≈ $15 2
- Aluminium heatsinks: ≈ $10
- mini fans (1.5 V): ≈ $5
- Aquarium pump (12 V DC): ≈ $10
- 1 g Al_2O_3 nanoparticles ≈ $4
- 1 g CuO nanoparticles: ≈ $2.6
- 1 L of water: Negligible cost.
- 12 V DC power supply: ≈ $15
- Total Material Cost: ≈ $101.6
- Energy unit cost: $0.15 kWh^{-1}

Other Inputs:

- System Life: Assume 15 years.
- Operating and Maintenance Costs: One of the most important advantages of TEC systems is that maintenance costs are very low. However, considering that moving parts such as fans and pumps used in the system may change, let us assume the annual operating and maintenance cost of the system is $20.
- Discount Rate: It is assumed to be 10%.
- Scrap Value: It is assumed that the scrap value is negligible at the end of the system's life.

As stated in "Cooling effect and COP assessment for TEC vaccine refrigerator" section, when water is used as the coolant, the system drops to 4 °C after 1200 s. Since the designed system is for portal vaccine refrigerator applications, it is evaluated that the daily operating period is 12 h, and it works for 365 days. During this process, it consumes 12 V 6 A power until it drops to 4 °C. When nanofluid is used as the coolant, it drops to 4 °C after 990 s and then it works for 12 h and 365 days a day. During this process, it consumes 12 V 5.3 A power until it drops to 4 °C. In both cases, it is assumed that 60% of the power is consumed to keep the cabinet temperature constant at 4 °C.

- **Energy Consumption Calculation**:

For water-cooled system:

Time to reach 4 °C: 1200 s = 1200/3600 h = 0.33 h.

Energy consumed while reaching 4 °C: 12 V * 6A * 0.33 h = 23.76 Wh.

Daily continuous operation: 12 h.

Energy consumed while working continuously: 12 V * 6A * 12 h * 60% = 432 Wh.

Total daily energy consumption: 23.76 Wh + 432 Wh = 455.76 Wh = 0.45576 kWh.

Annual energy consumption: 0.45576 kWh day^{-1} * 365 days = 166.34 kWh.

For CuO–Al_2O_3/water hybrid nanofluid-cooled system:

Time to reach 4 °C: 990 s = 990/3600 h = 0.275 h.

Energy consumed when reaching 4 °C: 12 V * 5.3A * 0.275 h = 17,595 Wh.

Daily continuous operation: 12 h.

Energy consumed when operating continuously: 12 V * 5.3A * 12 h * 60% = 383.04 Wh.

Total daily energy consumption: 17,595 Wh + 383.04 Wh = 400.64 Wh = 0.40064 kWh.

Annual energy consumption: 0.40064 kWh day^{-1} * 365 days = 146.23 kWh.

- **Annual Energy Cost Calculation:**

For water cooled: 166.34 kWh * $0.15 kWh^{-1} = $24.95 $year^{-1}$.

For CuO–Al_2O_3/water hybrid nanofluid-cooled system: 146.23 kWh * $0.15 kWh^{-1} = $21.93 $year^{-1}$.

- **Total Annual Operating Cost:**

For water cooled: $24.95 + $20 (maintenance) = $44.95 $year^{-1}$.

For $CuO–Al_2O_3$/water hybrid nanofluid-cooled system: \$21.93 + \$20 (maintenance) = \$41.93 $year^{-1}$.

- **Discounted Cost Calculation (15 years, 10% discount rate):**

For water cooled:

$$\sum_{t=1}^{15} \frac{44.95}{(1+0.1)^t} = \$376.65$$

For $CuO–Al_2O_3$/water hybrid nanofluid-cooled system:

$$\sum_{t=1}^{15} \frac{41.93}{(1+0.1)^t} = \$351.38$$

- **Total LCCA Calculation:**

For water cooled: \$95 (investment) + \$376.65 (operation) = \$471.65.

For $CuO–Al_2O_3$/water hybrid nanofluid-cooled system: \$101.6 (investment) + \$351.38 (business) = \$452.98.

The energy consumption and life cycle cost comparisons of the systems are shown in Figs. 11 and 12, respectively.

As a result, the system using $CuO–Al_2O_3$/water hybrid nanofluid is slightly more advantageous in terms of total life cycle cost. The use of $CuO–Al_2O_3$/water hybrid provides cost savings in the long term by reducing energy consumption as shown in Fig. 13.

Although the system draws a lower current when $CuO–Al_2O_3$/water hybrid nanofluid is used as the coolant, the difference is small. The current drawn from the power supply in Peltier elements varies depending on the voltage value and the temperature difference between the surfaces.

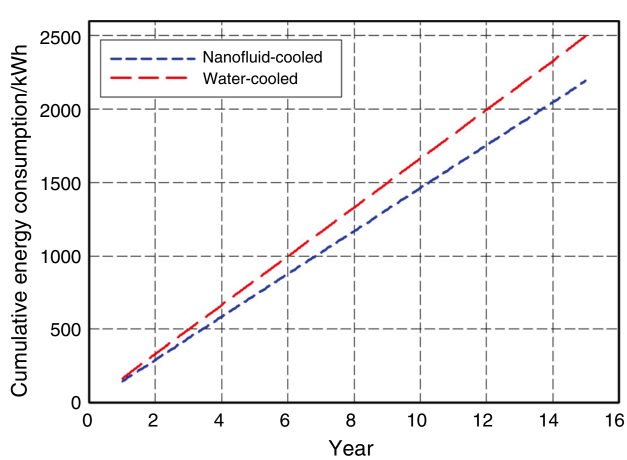

Fig. 11 Comparison of cumulative energy consumption

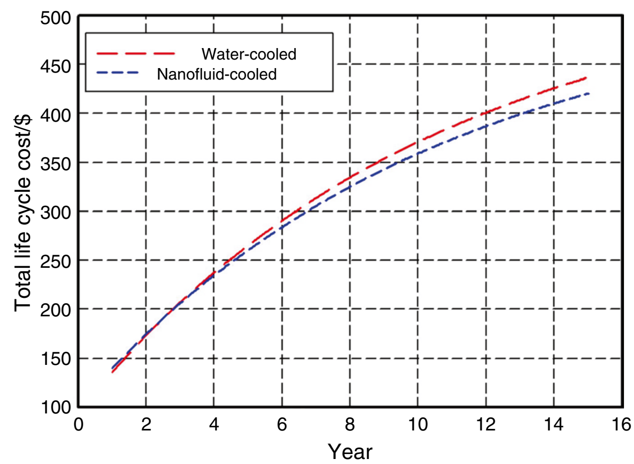

Fig. 12 Comparison of total life cycle cost

Constant and the same voltage were applied for both cases during the experiments. For this reason, the factor that determines the current values is the temperature difference between the surfaces. In addition, although nanofluid is used as a cooling fluid, due to the structure of Peltier devices, the temperature difference between the surfaces cannot exceed certain values. For this reason, the performances of the systems are similar to each other.

Carbon footprint assessment for TEC vaccine refrigerator

Considering the average use of fossil fuels and a mix of renewable energy in electricity generation, a typical carbon emission factor for a grid is around 0.5–0.6 kg CO_2 kWh^{-1}, a value close to the general world average and emissions in many developed countries [49, 50].

$$\text{CarbonEmission}\left(\text{kgCO}_2\right) = \text{AnnualEnergyConsumption(kWh)} \times \text{EmissionFactor}$$

$$\text{Total Carbon Footprint}\left(\text{kgCO}_2\right) = \sum_{t=1}^{15} \text{Annual emission}\left(\text{kgCO}_2\right)$$

For water-cooled system: Annual energy consumption 166.34 kWh.

$CuO–Al_2O_3$/water hybrid nanofluid-cooled system: Annual energy consumption 146.23 kWh. Emission factor: 0.6 kg CO_2 kWh^{-1}.

Equipment such as Peltier elements, fans and pumps may lose performance over time, which may increase energy consumption. For this reason, to make the results more realistic, we can assume that energy consumption increases by 1%. In addition, as the share of electricity production from

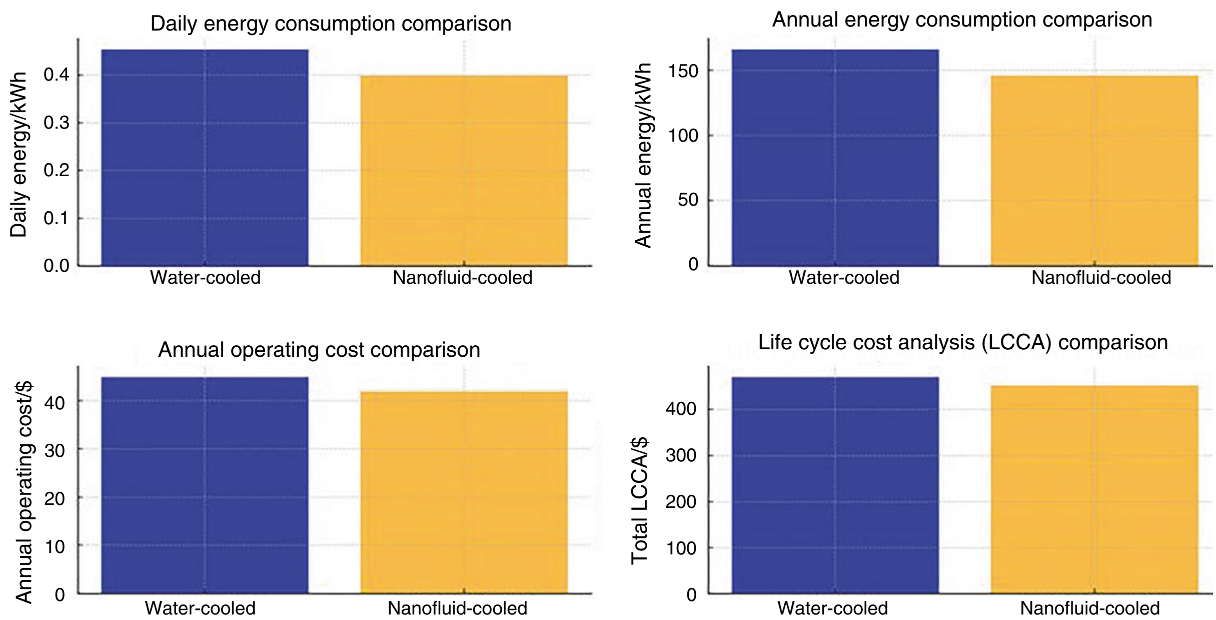

Fig. 13 Performance comparisons of vaccine refrigerator systems

renewable energy sources in total electricity production increases, the carbon emission factor is expected to decrease. For this reason, we can assume that the carbon emission factor decreases by 1% each year. Considering these data, the carbon emission values obtained for the 15-year period are shown in Table 3. In addition, the total carbon emission amounts for water-cooled and nanofluid-cooled cases are compared in Fig. 14.

According to the results, the CuO–Al_2O_3/water hybrid nanofluid-cooled system causes approximately 184.68 kg less CO_2 emissions and causes less damage to the environment. This system is a more environmentally friendly option compared to the water-cooled system in terms of both annual and cumulative carbon emissions due to lower energy consumption. In particular, the 12.3% lower carbon emissions over a 15-year lifespan are a significant gain in

Table 3 Carbon emission values obtained for the 15-year period

Year	Emission factor/kg CO_2/kWh	Water-cooled system			Nanofluid-cooled system		
		Energy cons./kWh	Emission/kg CO_2	Cumulative emission/kg CO_2	Energy cons./kWh	Emission/kg CO_2	Cumulative emissions/kg CO_2
1	0.594	168.0034	99.79402	99.79402	147.6923	87.72923	87.72923
2	0.58806	169.6834	99.78404	199.5781	149.1692	87.72045	175.4497
3	0.582179	171.3803	99.77406	299.3521	150.6609	87.71168	263.1614
4	0.576358	173.0941	99.76408	399.1162	152.1675	87.70291	350.8643
5	0.570594	174.825	99.75411	498.8703	153.6892	87.69414	438.5584
6	0.564888	176.5733	99.74413	598.6144	155.2261	87.68537	526.2438
7	0.559239	178.339	99.73416	698.3486	156.7784	87.6766	613.9204
8	0.553647	180.1224	99.72418	798.0728	158.3461	87.66783	701.5882
9	0.54811	181.9236	99.71421	897.787	159.9296	87.65907	789.2473
10	0.542629	183.7428	99.70424	997.4912	161.5289	87.6503	876.8976
11	0.537203	185.5803	99.69427	1097.186	163.1442	87.64154	964.5391
12	0.531831	187.4361	99.6843	1196.87	164.7756	87.63277	1052.172
13	0.526513	189.3104	99.67433	1296.544	166.4234	87.62401	1139.796
14	0.521247	191.2035	99.66437	1396.209	168.0876	87.61525	1227.411
15	0.516035	193.1156	99.6544	1495.863	169.7685	87.60649	1315.018

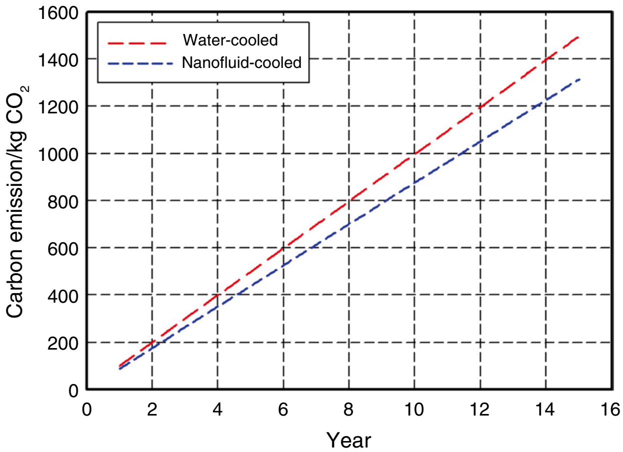

Fig. 14 Comparison of carbon emission amounts

terms of reducing environmental impacts. These results show how effective energy-efficient systems are in reducing carbon footprints. This indicates that the nanofluid cooling system is a better choice, especially for long-term environmental and economic sustainability goals.

It can be easily derived from the outputs of the research that CuO–Al_2O_3/water hybrid nanofluids driven thermoelectric vaccine refrigerators have a noticeable potential for effective minimisation of energy consumption and carbon footprint figures. It is useful to stress that the research phenomenon adopted in the present study is not limited to CuO–Al_2O_3 nanoparticles, and it can be easily expanded to various nanomaterials such as carbon nanotubes [51]. Moreover, the scope of the research problem can be related to the temperature control of Peltier surfaces through nanofluid-assisted PCM solutions [52].

Conclusions

The use of CuO–Al_2O_3/water hybrid nanofluid in thermoelectric vaccine refrigerators enhances heat dissipation, leading to reduced cooling times and lower energy consumption compared to water-cooled systems. The system's COP remains similar across both cooling fluids, as the temperature differences between the Peltier surfaces are nearly identical. However, the nanofluid-cooled system offers a significant environmental advantage by reducing carbon emissions by 12.3% over a 15-year lifespan. These results underscore the potential of nanofluid-based cooling systems for achieving long-term energy savings, environmental sustainability, and cost-efficiency in thermoelectric refrigeration applications. However, it is important to note that this study was conducted over a short-term period, and potential long-term issues such as nanoparticle sedimentation, corrosion, and thermal degradation were not investigated. While hybrid nanofluids generally offer better dispersion stability than single-component ones, further research is necessary to examine the ageing behaviour of the system under cyclic loading. Incorporating surfactants, using corrosion-resistant components, and applying periodic mixing can be potential solutions for future real-world applications. This study contributes to the development of greener and more efficient cooling technologies for critical applications such as vaccine storage.

Funding Open access funding provided by the Scientific and Technological Research Council of Türkiye (TÜBİTAK).

References

1. Navarro-Peris E, Corberan JM, Ancik Z. Evaluation of the potential recovery of compressor heat losses to enhance the efficiency of refrigeration systems by means of thermoelectric generation. Appl Therm Eng. 2015;89:755–62. https://doi.org/10.1016/j.applthermaleng.2015.06.033.
2. Cuce PM, Guclu T, Cuce E. Design, modelling, environmental, economic and performance analysis of parabolic trough solar collector (PTC) based cogeneration systems assisted by thermoelectric generators (TEGs). Sustain Energy Technol Assess. 2024;64:103745. https://doi.org/10.1016/j.seta.2024.103745.
3. Pourkiaei SM, et al. Thermoelectric cooler and thermoelectric generator devices: a review of present and potential applications, modeling and materials. Energy. 2019;186:115849. https://doi.org/10.1016/j.energy.2019.07.179.
4. Ayşe Pınar M, Tamer G, Erdem C. The effect of nanofluid usage on electricity consumption in thermoelectric refrigeration application: an experimental study. Gazi J Eng Sci. 2022;8(2):228–36. https://doi.org/10.30855/gmbd.0705006.
5. Guclu T, Cuce E. Thermoelectric coolers (TECs): from theory to practice. J Electron Mater. 2019;48(1):211–30. https://doi.org/10.1007/s11664-018-6753-0.
6. Zaferani SH, Sams MW, Ghomashchi R, Chen ZG. Thermoelectric coolers as thermal management systems for medical applications: design, optimization, and advancement. Nano Energy. 2021;90:106572. https://doi.org/10.1016/j.nanoen.2021.106572.
7. Nazari S, Safarzadeh H, Bahiraei M. Performance improvement of a single slope solar still by employing thermoelectric cooling channel and copper oxide nanofluid: an experimental study. J Clean Prod. 2019;208:1041–52. https://doi.org/10.1016/j.jclepro.2018.10.194.
8. Yu J, Wang B. Enhancing the maximum coefficient of performance of thermoelectric cooling modules using internally

cascaded thermoelectric couples. Int J Refrig. 2009;32(1):32–9. https://doi.org/10.1016/j.ijrefrig.2008.08.006.

9. Gokcek M, Sahin F. Experimental performance investigation of minichannel water cooled-thermoelectric refrigerator. Case Stud Therm Eng. 2017;10:54–62. https://doi.org/10.1016/j.csite.2017.03.004.
10. Xu RJ, Zhao YQ, Chen H, Wu QP, Yang LW, Wang HS. Numerical and experimental investigation of a compound parabolic concentrator-capillary tube solar collector. Energy Convers Manag. 2020;204:112218. https://doi.org/10.1016/j.enconman.2019.112218.
11. Afshari F. Experimental and numerical investigation on thermoelectric coolers for comparing air-to-water to air-to-air refrigerators. J Therm Anal Calorim. 2021;144(3):855–68. https://doi.org/10.1007/s10973-020-09500-6.
12. Huang HS, Weng YC, Chang YW, Chen SL, Ke MT. Thermoelectric water-cooling device applied to electronic equipment. Int Commun Heat Mass Transf. 2010;37(2):140–6. https://doi.org/10.1016/j.icheatmasstransfer.2009.08.012.
13. Afshari F, Ceviz MA, Manay E, Ceylan M, Muratçobanoğlu B. Performance analysis of air-to-water binary thermoelectric Peltier cooling systems and determination of optimum arrangement. J Braz Soc Mech Sci Eng. 2022;44(9):1–18. https://doi.org/10.1007/s40430-022-03737-y.
14. Pathak PK, Boriwal L, Anand N. Performance analysis of water cooled thermoelectric module TEC-12715. *Unpublished report*. 2017.
15. Cuce E, Cuce PM, Guclu T, Besir AB. On the use of nanofluids in solar energy applications. J Therm Sci. 2020;29(3):513–34. https://doi.org/10.1007/s11630-020-1269-3.
16. Özerinç S, Kakaç S, Yazıcıoğlu AG. Enhanced thermal conductivity of nanofluids: a state-of-the-art review. Microfluid Nanofluidics. 2010;8(2):145–70. https://doi.org/10.1007/s10404-009-0524-4.
17. Sohel MR, Khaleduzzaman SS, Saidur R, Hepbasli A, Sabri MFM, Mahbubul IM. An experimental investigation of heat transfer enhancement of a minichannel heat sink using Al_2O_3–H_2O nanofluid. Int J Heat Mass Transf. 2014;74:164–72. https://doi.org/10.1016/j.ijheatmasstransfer.2014.03.010.
18. Syam Sundar L, Venkata Ramana E, Singh MK, Sousa ACM. Thermal conductivity and viscosity of stabilized ethylene glycol and water mixture Al_2O_3 nanofluids for heat transfer applications: an experimental study. Int Commun Heat Mass Transf. 2014;56:86–95. https://doi.org/10.1016/j.icheatmasstransfer.2014.06.009.
19. Alawi OA, Sidik NAC, Xian HW, Kean TH, Kazi SN. Thermal conductivity and viscosity models of metallic oxides nanofluids. Int J Heat Mass Transf. 2018;116:1314–25. https://doi.org/10.1016/j.ijheatmasstransfer.2017.09.133.
20. Pryazhnikov MI, Minakov AV, Rudyak VY, Guzei DV. Thermal conductivity measurements of nanofluids. Int J Heat Mass Transf. 2017;104:1275–82. https://doi.org/10.1016/j.ijheatmasstransfer.2016.09.080.
21. Elibol EA, Yilmazoglu MZ, Aksoy AE, Aktas F. Thermal analysis of a refrigeration system integrated with a thermoelectric couple and microchannels using TiO_2–water nanofluid. Int J Heat Fluid Flow. 2024;108:109491. https://doi.org/10.1016/j.ijheatfluidflow.2024.109491.
22. Cuce E, Guclu T, Cuce PM. Improving thermal performance of thermoelectric coolers (TECs) through a nanofluid driven water to air heat exchanger design: an experimental research. Energy Convers Manag. 2020;214:112893. https://doi.org/10.1016/j.enconman.2020.112893.
23. Cuce PM, Cuce E, Guclu T, Shaik S, Alshahrani S, Saleel CA. Effect of using hybrid nanofluids as a coolant on the thermal performance of portable thermoelectric refrigerators. Sustain Energy Technol Assess. 2022;53:102685. https://doi.org/10.1016/j.seta.2022.102685.
24. Mohammadian SK, Zhang Y. Analysis of nanofluid effects on thermoelectric cooling by micro-pin-fin heat exchangers. Appl Therm Eng. 2014;70(1):282–90. https://doi.org/10.1016/j.applthermaleng.2014.05.010.
25. Ahammed N, Asirvatham LG, Wongwises S. Thermoelectric cooling of electronic devices with nanofluid in a multiport minichannel heat exchanger. Exp Therm Fluid Sci. 2016;74:81–90. https://doi.org/10.1016/j.expthermflusci.2015.11.023.
26. Duan L, Han J, Cao L, Huo C. Experimental study on heat transfer characteristics of CNTs/ Al_2O_3 nanofluids in personal cooling system based on thermoelectric refrigeration. Procedia Eng. 2017;205:588–95. https://doi.org/10.1016/j.proeng.2017.10.421.
27. Elibol EA. Performance analysis of a refrigeration system integrated with a thermoelectric cooler and microchannels in terms of heat transfer using a hybrid nanofluid. Appl Therm Eng. 2024;250:123465. https://doi.org/10.1016/j.applthermaleng.2024.123465.
28. Barbes B, Paramo R, Blanco E, Casanova C. Thermal conductivity and specific heat capacity measurements of CuO nanofluids. J Therm Anal Calorim. 2014;115(2):1883–91. https://doi.org/10.1007/s10973-013-3518-0.
29. Khedkar RS, Sonawane SS, Wasewar KL. Influence of CuO nanoparticles in enhancing the thermal conductivity of water and monoethylene glycol based nanofluids. Int Commun Heat Mass Transf. 2012;39(5):665–9. https://doi.org/10.1016/j.icheatmasstransfer.2012.03.012.
30. Senthilraja S, Vijayakumar K, Gangadevi R. A comparative study on thermal conductivity of Al_2O_3/water, CuO/water and Al_2O_3–CuO/water nanofluids. Dig J Nanomater Biostruct. 2015;10(4):1449–58.
31. Esfe MH, Saedodin S, Mahian O, Wongwises S. Thermal conductivity of Al_2O_3/water nanofluids: measurement, correlation, sensitivity analysis, and comparisons with literature reports. J Therm Anal Calorim. 2014;117(2):675–81. https://doi.org/10.1007/s10973-014-3771-x.
32. Nanografi. No Title. https://www.nanografi.com.
33. Liu H, Li G, Zhao X, Ma X, Shen C. Investigation of the impact of the thermoelectric geometry on the cooling performance and thermal–mechanic characteristics in a thermoelectric cooler. Energy. 2023;267:126471. https://doi.org/10.1016/j.energy.2022.126471.
34. Amidu MA, Addad Y, Riahi MK, Abu-Nada E. Numerical investigation of nanoparticles slip mechanisms impact on the natural convection heat transfer characteristics of nanofluids in an enclosure. Sci Rep. 2021;11:15678. https://doi.org/10.1038/s41598-021-95269-z.
35. Cao Y, Hamdi A, Jarad F, et al. MHD natural convection nanofluid flow in a heat exchanger: effects of Brownian motion and thermophoresis for nanoparticles distribution. Case Stud Therm Eng. 2021;28:101394. https://doi.org/10.1016/j.csite.2021.101394.
36. Chen WY, Shi XL, Zou J, Chen ZG. Thermoelectric coolers: progress, challenges, and opportunities. Small Methods. 2022;6(2):2101235. https://doi.org/10.1002/smtd.202101235.
37. Kaiprath J, Kumar VKV. A review on solar photovoltaic-powered thermoelectric coolers, performance enhancements, and recent advances. Int J Air Cond Refrig. 2023;31(1):1–30. https://doi.org/10.1007/s44189-023-00022-y.
38. Woodward DG. Life cycle costing—theory, information acquisition and application. Int J Proj Manag. 1997;15(6):335–44. https://doi.org/10.1016/s0263-7863(96)00089-0.
39. U.S. Department of Energy. Life cycle cost manual for the Federal Energy Management Program, 2020. https://www.energy.gov/eere/femp/downloads/life-cycle-costing-manual.

40. Vendrusculo EA, Queiroz GC, Jannuzzi GDM, da Silva HX, Pomilio JA. Life cycle cost analysis of energy efficiency design options for refrigerators in Brazil. Energy Effic. 2009;2(3):271–86. https://doi.org/10.1007/s12053-008-9034-6.
41. Kishita Y, Ohishi Y, Uwasu M, Kuroda M, Takeda H, Hara K. Evaluating the life cycle CO_2 emissions and costs of thermoelectric generators for passenger automobiles: a scenario analysis. J Clean Prod. 2016;126:607–19. https://doi.org/10.1016/j.jclepro.2016.03.129.
42. Rugani B, Vázquez-Rowe I, Benedetto G, Benetto E. A comprehensive review of carbon footprint analysis as an extended environmental indicator in the wine sector. J Clean Prod. 2013;54:61–77. https://doi.org/10.1016/j.jclepro.2013.04.036.
43. Cascini A, Gamberi M, Mora C, Rosano M, Bortolini M. Comparative carbon footprint assessment of commercial walk-in refrigeration systems under different use configurations. J Clean Prod. 2016;112:3998–4011. https://doi.org/10.1016/j.jclepro.2015.08.075.
44. Li Z, et al. Trends in research on the carbon footprint of higher education: a bibliometric analysis (2010–2019). J Clean Prod. 2021;289:125642. https://doi.org/10.1016/j.jclepro.2020.125642.
45. Moffat RJ. Uncertainty analysis. In: Azar K, Azar K, editors. Thermal measurements in electronic cooling. CRC Press; 2020. p. 45–80. https://doi.org/10.1201/9781003067948-2.
46. Cuce PM. Design and experimental investigation of a thermoelectric vaccine cabinet integrated with photovoltaic and nanofluids. J Therm Anal Calorim. 2024;149(17):9955–65. https://doi.org/10.1007/s10973-024-13433-9.
47. Vangroenweghe F. Good vaccination practice: it all starts with a good vaccine storage temperature. Porc Health Manag. 2017;3(1):1–7. https://doi.org/10.1186/s40813-017-0071-4.
48. Weltermann BM, Markic M, Thielmann A, Gesenhues S, Hermann M. Vaccination management and vaccination errors: a representative online-survey among primary care physicians. PLoS ONE. 2014;9(8):e105119. https://doi.org/10.1371/journal.pone.0105119.
49. International Energy Agency. CO_2 emissions from fuel combustion. *IEA Reports*. Accessed Nov 22, 2024. https://www.iea.org/reports/co2-emissions-from-fuel-combustion-2020.
50. The Carbon Trust. Sustainability guides, reports, and videos. *The Carbon Trust*. Accessed Nov 22, 2024. https://www.carbontrust.com/our-work-and-impact/guides-reports-and-videos.
51. Vigneshwaran P, Saboor S, Suresh S, Abbas M, Saleel CA, Cuce E. Solar salt with carbon nanotubes as a potential phase change material for high-temperature applications: investigations on thermal properties and chemical stability. ACS Omega. 2023;8(20):17563–72.
52. Roy A, Venkitaraj KP, Vigneshwaran P, Saboor S, Cuce E, Saxena KK. Enhanced convective heat transfer with Al_2O_3-water nanofluid in a PCM-based thermal energy storage system. J Energy Storage. 2024;97:112853.